Enhanced Sensing of Nonpolar Volatile Organic Compounds by Silicon Nanowire Field Effect Transistors

Yair Paska,[†] Thomas Stelzner,[‡] Silke Christiansen,[‡,§] and Hossam Haick[†,*]

[†]The Department of Chemical Engineering and Russell Berrie Nanotechnology Institute, Technion—Israel Institute of Technology, Haifa 32000, Israel, [‡]Institute of Photonic Technology e.V., Albert-Einstein-Strasse 9, 07745 Jena, Germany, and [§]Max-Planck-Institute for the Science of Light, Günther-Scharowsky-Strasse 1, 91058 Erlangen, Germany

ABSTRACT Silicon nanowire field effect transistors (Si NW FETs) are emerging as powerful sensors for direct detection of biological and chemical species. However, the low sensitivity of the Si NW FET sensors toward nonpolar volatile organic compounds (VOCs) is problematic for many applications. In this study, we show that modifying Si NW FETs with a silane monolayer having a low fraction of Si—O—Si bonds between the adjacent molecules greatly enhances the sensitivity toward nonpolar VOCs. This can be explained in terms of an *indirect* sensor—VOC interaction, whereby the nonpolar VOC molecules induce conformational changes in the organic monolayer, affecting (i) the dielectric constant and/or effective dipole moment of the organic monolayer and/or (ii) the density of charged surface states at the SiO_2/monolayer interface. In contrast, polar VOCs are sensed directly *via* VOC-induced changes in the Si NW charge carriers, most probably due to electrostatic interaction between the Si NW and polar VOCs. A semiempirical model for the VOC-induced conductivity changes in the Si NW FETs is presented and discussed.

KEYWORDS: silicon · nanowire · transistor · sensor · volatile organic compound · nonpolar

Silicon nanowires (Si NWs) offer unique opportunities for signal transduction associated with moderately selective recognition of chemical and biological species.[1−3] Oxide-coated Si NW field effect transistors (FETs) were functionalized with amino siloxanes to impart relatively high sensitivity toward pH and with a variety of biological receptors to impart selectivity toward biological species in solution.[1,3−5] Similar approaches were used for achieving highly sensitive detection of polar analytes in the gas phase (N_2O, NO, CO, *etc.*).[4] However, the detection of nonpolar volatile organic compounds (VOCs) still remains challenging (*cf.* refs 6−8). For example, Si NW FETs exhibited detection limits down to 20 ppb NO, but the same devices responded weakly to 1000 ppm hexane (a nonpolar VOC)[4] and showed no response to 40 ppb hexane. The low sensitivity toward nonpolar analytes can in principle be improved by modifying the Si NW surface with appropriate organic receptors. For example, oxide-coated Si NW FETs modified with alkane-silanes, aldehyde-silanes, or amino-silanes showed an improved response and sensitivity when exposed to hexane at 1000 ppm. Unfortunately, these improvements are still far away from those required for successful applications in different branches of industry, homeland security, environmental monitoring, and medicine.[1,6,7]

The limited sensitivity of the Si NW FET sensors toward nonpolar VOCs could be attributed to four main reasons. The first reason is the weak adsorption of nonpolar VOCs in molecule-free sites; silane (or other) molecules can cover as much as 50% of the SiO_2 surface sites (*i.e.*, number of silane molecules divided by the number of exposed atoms on the surface). This relatively poor coverage leaves plenty of molecule-free sites and, also, nanometric pinholes that can directly be occupied by all sorts of VOCs, essentially and most effectively by polar ones (due to the hydrophilic nature of SiO_2). The second reason is the lack of suitable nonpolar organic functionalities that can be attached to the Si NWs. A recent study has shown that nonpolar gases transfer more energy to nonpolar surface functional groups (9.2 kJ/mol) than to the polar ones (6.9 kJ/mol) and *vice versa*.[9] The third reason is the high density of surface states at the SiO_2/Si interface.[10] The presence of native SiO_2 at the Si NW surface is responsible for interface states that lower the sensitivity of the FET device in a sense that the FET does not react efficiently to manipulations of gate (or molecular gating) voltage[11,12] Several studies have shown that removing the oxide and attaching an organic monolayer directly to the Si surface, through chemical (*e.g.*, Si—C) bonds, increases the trans-conductance values and allows the formation of Si NW FETs with higher on—off ratios, as

* Address correspondence to hhossam@technion.ac.il.

Received for review March 29, 2011 and accepted June 1, 2011.

Published online June 07, 2011
10.1021/nn201184c

© 2011 American Chemical Society

TABLE 1. Physical Properties of the Analytes Used for the Exposure Experiments[29]

analyte	P_0[a] (Torr)	ε_v[b]	dipole (D)	volume (Å^3)	formula
n-hexane	150	1.88	0	113.0	$CH_3(CH_2)_4CH_3$
n-octane	14	1.94	0	146.6	$CH_3(CH_2)_6CH_3$
n-decane	1.4	1.98	0	180.2	$CH_3(CH_2)_8CH_3$
water	32	80.1	1.85	19.3	H—OH
ethanol	59	25.3	1.63	54.0	CH_3CH_2—OH
butanol	4	17.8	1.7	87.6	$CH_3(CH_2)_3$—OH
hexanol	1	13.0	2.48	121.2	$CH_3(CH_2)_5$—OH

[a] P_0 stands for the analyte's vapor pressure at 25 °C. [b] ε_v stands for the dielectric constant of the analyte at 20 °C.

compared to SiO_2—Si NW FETs[11−13] (*cf.* also refs 14 and 15). Nevertheless, there are practical and technical limitations to these approaches, including, but not confined to, the poor oxidation resistance[12,16,17] and the complexity of the functionalization procedure, especially when the Si NWs are already integrated in a device platform. The fourth reason is the high density of trap states at the air/SiO_2 interface. The presence of native SiO_2 at the Si NW surface is responsible for surface trap states (SiO^-) that cause "hysteresis", namely, a lag in the response obtained in the forward and backward electrical scans of the source−drain current (I_{ds}) *versus* gate voltage (V_{gs}). These species serve as sorption sites for water molecules,[18] thus severely hindering the device/sensor performance.

In this paper, we show that attaching appropriate, dense hydrophobic organic hexyltrichlorosilane (HTS) monolayers that passivate most of the SiO_2/Si NW surface trap states in a FET device could serve as a successful and simple strategy to achieve and maintain high sensitivity toward nonpolar VOCs. A semi-empirical model that describes the conductivity change upon exposure to nonpolar VOCs will be presented.

RESULTS AND DISCUSSION

The effect of HTS monolayer on the sensing characteristics was studied by exposing the functionalized and pristine Si NW FETs to a number of polar and nonpolar VOCs in the gas phase (see Table 1). Figure 1 shows a schematic representation and an image of a representative Si NW FET test device that was modified with a 0% cross-linked HTS monolayer (*i.e.*, a HTS monolayer that has the lowest possible fraction of Si—O—Si bonds between the adjacent molecules).[19−21] Figure 2 shows the source−drain current (I_{ds}) *versus* gate voltage (V_{gs}) characteristics of a typical test device during exposure to different concentrations of octane and decane, as representative examples for nonpolar VOCs. The observed I_{ds} at high negative V_{gs} was almost equal to I_{ds} in air. I_{ds} systematically decreased upon applying positive gate voltages and increasing the VOC

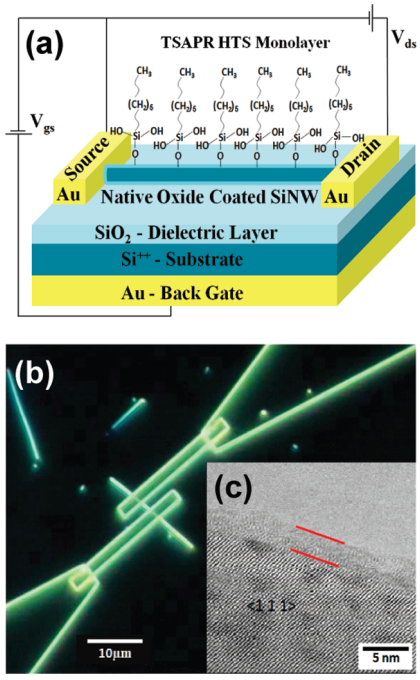

Figure 1. (a) Schematics of a back gate Si NW FET configuration. (b) Optical microscopy image of a representative Si NW FET. (c) TEM image of a representative Si NW having ~5 nm native oxide on its surface.

concentration. Based on these data the threshold voltage (V_{th}) was extracted from the extrapolation of the linear part of the I_{ds}−V_{gs} and the hole mobility (μ_h) was extracted using the following relationship:[22]

$$\mu_h = \frac{dI_{ds}}{dV_{gs}} \frac{\ln\{(2d_{ox} + R_{NW})/R_{NW}\}}{2\pi\varepsilon_{ox}} \frac{L_{NW}}{V_{ds}} \quad (1)$$

where d_{ox} is the width of the gate oxide, ε_{ox} is the dielectric constant of the oxide, R_{NW} is the radius of the Si NW, and L_{NW} is the length of the channel. A linear increase of the V_{th} and μ_h was observed with the VOC concentration, as shown in the upper insets of Figure 2. Exposure to equivalent polar VOCs and water molecules (*cf.* Table 1) led to significantly different responses. Indeed, the I_{ds}−V_{gs} response of the HTS-Si NW FET at high negative gate voltages exhibited, respectively, higher and lower currents than the constituent base responses upon exposure to polar VOCs (ethanol, butanol, and hexanol) and water molecules (see Figure 3). At positive gate voltages, the I_{ds}−V_{gs} response showed no differences between the pre-exposure and post-exposure signals to polar VOCs and water molecules. Exceptional was hexanol, which led to lower I_{ds}−V_{gs} responses during the exposure process. For all polar species, V_{th} and μ_h exhibited a proportional linear correlation with the VOC concentrations (not shown).

The conductivity response of the HTS-Si NW FET sensors was calculated according to $\Delta G/G_0 = (G - G_0)/G_0$ where G is the steady-state conductivity of the

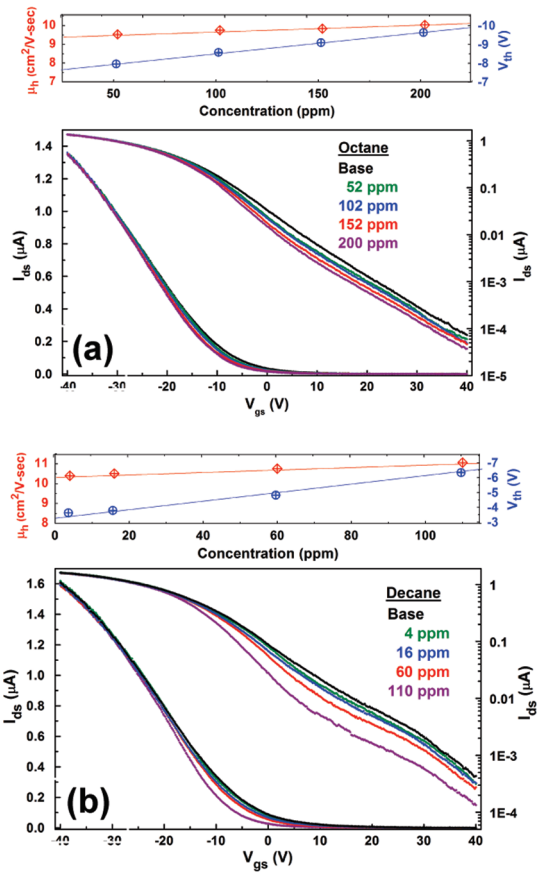

Figure 2. Linear-scale (left *y*-axis) and logarithmic-scale (right *y*-axis) presentations of $I_{ds}-V_{gs}$ measurements with various concentrations of (a) octane and (b) decane. The upper insets of panels (a) and (b) present V_{th} (blue circles) and μ_h (red rhombus) as a function of the concentration of octane and decane, respectively.

sensor upon exposure to VOC and G_0 is the baseline conductivity of the sensor in the absence of analyte. Figure 4 shows the $\Delta G/G_0$ of a HTS-Si NW FET sensor for different concentrations of octane and decane, as representative examples. As could be seen in the figure, the $\Delta G/G_0$ values were zero at high negative gate voltages and were negative at positive back gate voltages. For the latter, $\Delta G/G_0$ was almost constant after a given back gate threshold. Figure 5 summarizes the $\Delta G/G_0$ values calculated for the same HTS-Si NW FET sensors toward all polar and nonpolar VOCs studied here. As could be seen in the figure, all polar VOCs showed a nonzero positive conductivity change at high negative voltages and a maximum close to the base V_{th}. In contrast, the water molecules showed a nonzero negative conductivity change at high negative voltages and a minimum close to the base V_{th}. The sensitivity of the HTS-Si NW FET sensor toward nonpolar VOCs exceeded the sensitivity toward polar molecules. For example, at a $V_g \approx 0$ the sensor responses to ~55 ppm hexane, ~55 ppm octane, and ~60 ppm decane were about −5%, −25%, and −45%, respectively. At the same gate voltage, the responses to ~25 000 ppm water, ~60 ppm ethanol, and ~50 ppm butanol were about −20%, +5%, and +30%, respectively (see Supporting Information, Table 1S). This behavior could be attributed to the formation of a dense HTS monolayer[19−21] that acts by transferring the recognition event of the nonpolar VOCs to the Si NW while preventing polar molecules from reaching the Si NW surface. In support of this claim, we observed negligible responses of *pristine* Si NW FET sensors upon exposure to nonpolar VOCs and nonstable and nonreproducible responses upon exposure to polar VOCs, as summarized in the Supporting Information, Table 1S.

The observed electrical characteristics before and after exposure to VOCs indicate the involvement of two physical effects in the sensing process. The first effect could be ascribed to *direct* changes in the (volume) charge carriers inside the Si NWs, most probably due to electrostatic interaction between the Si NW and polar VOCs. This *direct* effect could be evidenced from the correlation between the Si NW response and the dipole moment of the VOC. More specifically: (i) nonpolar VOCs showed no response at high negative gate voltages and (ii) polar VOCs showed positive responses upon increasing their dipole moment. The second effect could be ascribed to *indirect* changes in one or a combination of the following parameters: (i) the dielectric constant of the organic monolayer; (ii) the effective dipole moment of the organic monolayer; and/or (iii) the charged surface-state density of the SiO_2/monolayer interface. This could be evidenced from the observation of negative responses at more positive gate voltage (*i.e.*, above the V_{th}) for larger VOC dimensions, whether having polar or nonpolar features. The weight of the *direct* and *indirect* effects in the sensing process depends on the VOC characteristics. As an illustrative example, one should mention the higher response of the HTS-Si NW FET for butanol, as compared to ethanol, at positive gate voltages. Since ethanol and butanol have similar dipole moments, but different chain length, the difference in the response could be attributed to the structural parameter. VOCs that have both longer chain length and stronger dipole moment, such as hexanol (Table 1), exhibited significantly more pronounced responses either at positive or at negative gate voltages. The opposite response sign but similar response shape of water could be attributed to the direction of the dipole moment when it interacts with the HTS monolayer. It is reasonable to assume that the water molecules diffuse into the HTS monolayer and reside close to the SiO_2 surface, while pointing the OH groups toward the SiO_2 coating of the Si NW. In contrast, polar VOCs interact with the HTS monolayer through the carbon chain, while pointing the OH groups out of the SiO_2 coating of the Si NW.

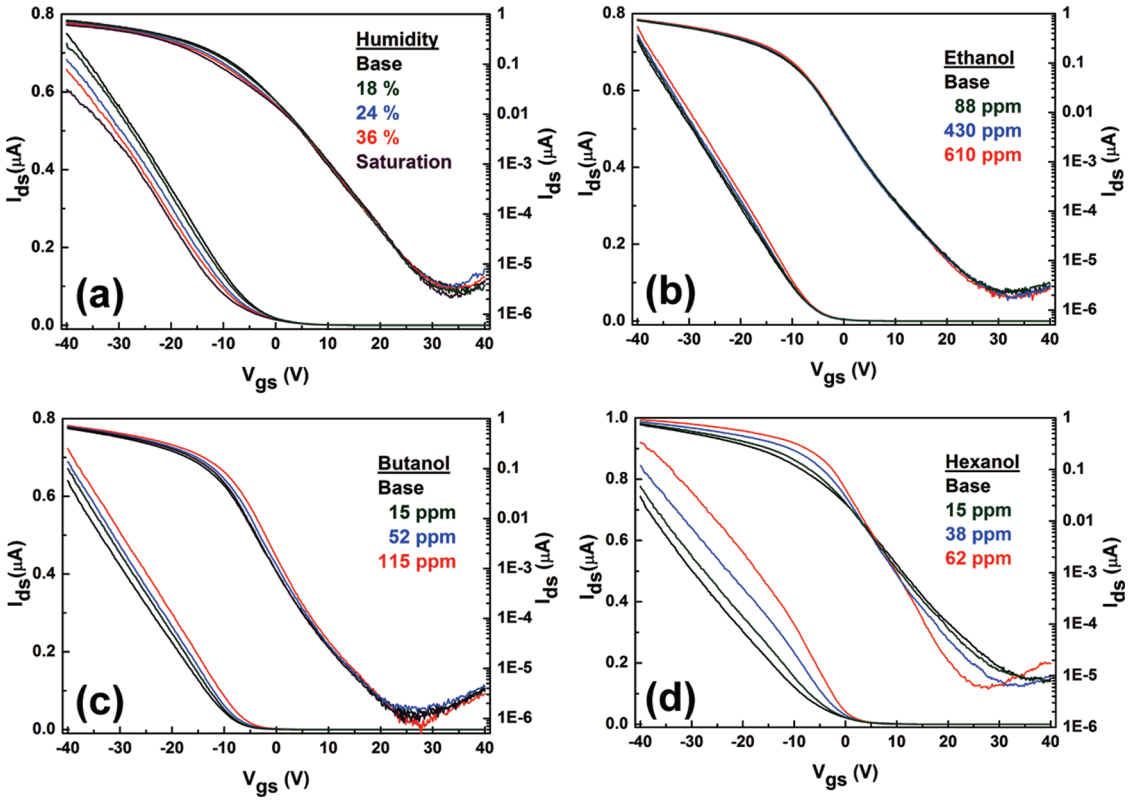

Figure 3. Linear-scale (left *y*-axis) and logarithmic-scale (right *y*-axis) presentations of $I_{ds}-V_{gs}$ measurements before and after exposure to (a) water, (b) ethanol, (c) butanol, and (d) hexanol at different concentrations.

The total conductivity in the Si NW FETs can be expressed through[18]

$$G = q\mu_h\left(n_h(V_{gs} - V_{th}) + \frac{2n_s}{R_{NW}}\right) \quad (2)$$

where q is the electron elementary charge, μ_h is the holes mobility, n_h is the hole volume density (*i.e.*, the holes accumulated by applying a voltage with a gate electrode), n_s is the negative charged surface-states density, and R_{NW} is the radius of the Si NW. Accordingly, $\Delta G/G_0$, originating from analyte adsorption, can be formulated as follows:

$$\frac{\Delta G}{G_0} = \frac{1}{\frac{R_{NW}}{2}\frac{n_{h0}(V_{gs} - V_{th})}{n_{s0}} + 1}\frac{\mu_h n_h(\Delta\varphi\{D\}) - \mu_{h0}n_{h0}}{2\mu_{h0}n_{s0}/R_{NW}} + \frac{1}{\frac{R_{NW}}{2}\frac{n_{h0}(V_{gs} - V_{th})}{n_{s0}} + 1}\frac{\mu_h n_s - \mu_{h0}n_{s0}}{\mu_{h0}n_{s0}} \quad (3)$$

where the index "0" stands for the absence of analyte (*i.e.*, baseline signal). As could be seen in eq 3, $\Delta G/G_0$ is composed of two main expressions. The first is ascribed to the *direct* effect, where the n_h is affected by the electric field (or potential, $\Delta\varphi$) induced by a physical adsorption of the nonideal layer of polar VOCs.[23] The magnitude and the sign of this conductivity change is proportional to the magnitude and direction of the VOC's dipole moment. We speculate that the maximum seen in the relative conductivity of polar VOCs near the V_{th} is related to the VOC polarizability in the presence of the gate field. For relatively large dimensions of polar VOCs, this effect might occur through change in the VOC orientation inside the adsorptive (HTS) monolayer. This speculation might explain the pronounced response of hexanol upon applying a positive gate voltage. The second expression is ascribed to the *indirect* effect, which consists of two main parts. The first part of this (second) expression is a prefactor (PF) that presents the ratio between the n_h and surface holes ($2n_{s0}/R_{NW}$, *i.e.*, holes induced by the negatively charged surface state). The second part of this (second) expression presents the relative change of the product of mobility multiplied by the charged surface-state density ($\Delta\mu_h n_s/\mu_{h0}n_{s0}$). According to this expression, $\Delta G/G_0$ approaches zero at high negative gate voltage (PF→0). Applying higher positive gate voltage increases the $\Delta G/G_0$ to a value that is equivalent to $\Delta\mu_h n_s/\mu_{h0}n_{s0}$, meaning that devices are most efficient at positive gate voltage, where the devices are almost turned off (*i.e.*, low hole volume density, PF→1).[24] Therefore, the observed minimum in Figure 4 is $\Delta\mu_h n_s/\mu_{h0}n_{s0}$. Extracting the normalized PF values showed a linear correlation with the VOC concentration (see upper insets in Figure 4a and b and Supporting Information, Table 2S).

Analysis of the sensing result *via* the PF revealed (i) the PF was independent of the type or concentration of the nonpolar VOC; (ii) the PF was independent of the μ_h or V_{th} of the device after exposure; (iii) the PF was

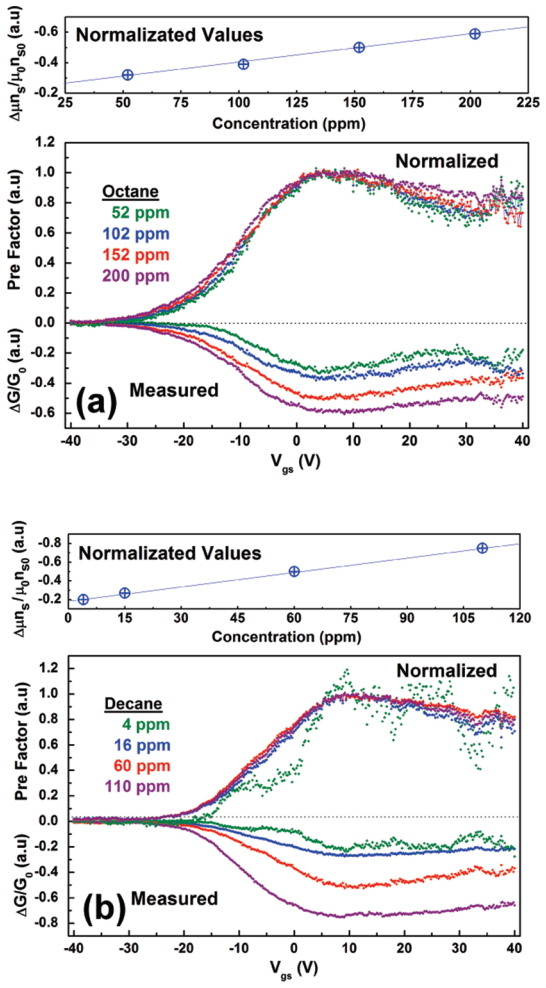

Figure 4. $\Delta G/G_0$ (lower part; measured) and prefactor (upper part; normalized) for different concentrations of (a) octane and (b) decane. Upper insets: The normalized values ($\Delta\mu_h n_s/\mu_{h0} n_{s0}$) as a function of concentration for (a) octane and (b) decane. The noisy conductivity at high positive voltages could be related to current changes on the order of the noise magnitude (*pA*). Noisy response also seems to occur near the limit of detection.

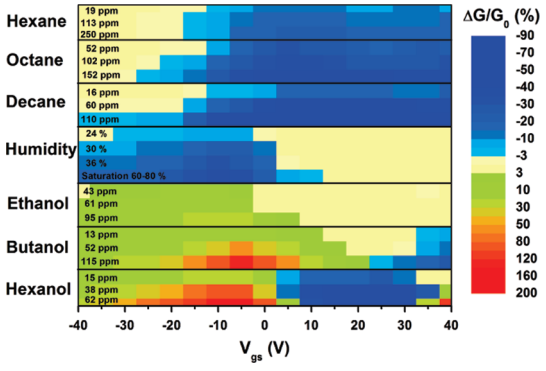

Figure 5. Counter map of the relative conductivity change at different gate voltages for the polar and nonpolar VOCs at different concentrations. In the case of hexanol, the gate voltage, where minority carrier (electrons) appears, shifts to a lower value and the relative conductivity change becomes positive (decrease of surface holes is equivalent to increase of surface electrons).

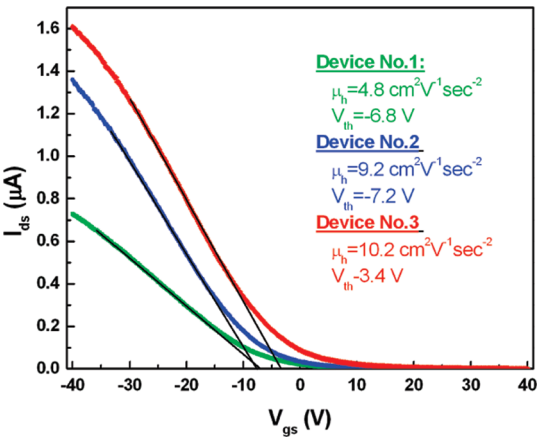

Figure 6. Base $I_{ds}-V_{gs}$ response of three HTS-Si NW FET devices. Devices 1 and 2 had the same V_{th0} but different μ_{h0} (see Supporting Information, Table 2S). Devices 2 and 3 had the same μ_{h0} but different V_{th0} (see Supporting Information, Table 2S).

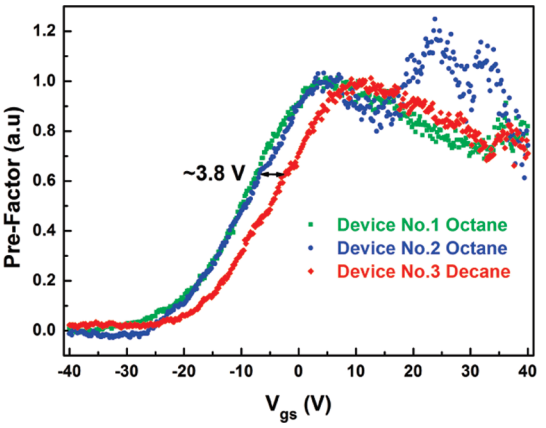

Figure 7. Calculated values of the prefactor (PF) of HTS-Si NW FET from three different devices having different electrical properties (see Figure 6 and Supporting Information, Table 2S). The PFs of devices 1 and 2, calculated upon exposure to octane, exhibited identical properties. The PF of device 3, calculated upon exposure to decane, had the same shape as device 1, but was shifted to a positive voltage by ~3.8 V. This shift is equal to the V_{th0} difference of the base devices.

characterized by an exponential shape at high negative voltages (see Supporting Information, Figure 1S); and (iv) the PF was dependent on the V_{th} of the base device (V_{th0}). With these findings in mind, we test our understanding by calculating the PF from three different HTS-Si NW FET devices: devices 1 and 2, which have the same V_{th0} but different μ_{h0}, and devices 2 and 3, which have similar μ_{h0} but different V_{th0} (see Figures 6 and 7 and Supporting Information, Table 2S). As can be seen from Figure 7, the PFs of devices 1 and 2 were identical, while the PF of device 3 was shifted by ~3.8 V to higher positive gate voltages. This shift is exactly equal to the V_{th0} difference of the base devices (between devices 3 and 1/2), thus confirming the validity of eq 3.

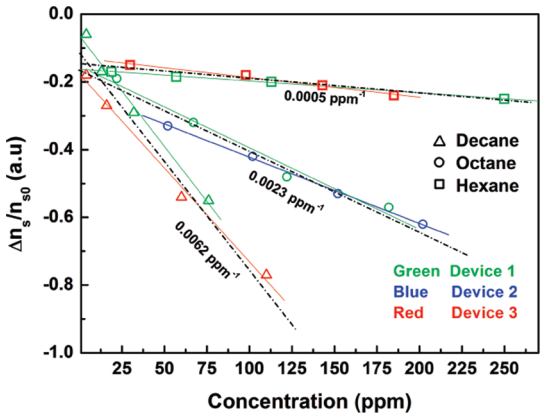

Figure 8. Relative surface-state density change ($\Delta n_s/n_{s0}$), as extracted from three different devices and three different nonpolar VOCs (hexane, octane, and decane). The $\Delta n_s/n_{s0}$ values were calculated using the relative change of the product of mobility multiplied by the surface-state density ($\Delta\mu_h n_s/\mu_{h0}n_{s0}$) and the mobility before (μ_{h0}) and after exposure (μ_h) to analytes.

According to the proposed model (eq 3), the type of nonpolar VOC manifests itself only in $\Delta\mu_h n_s/\mu_{h0}n_{s0}$. It seems that the most critical parameter for sensing the nonpolar VOCs is the interaction between the monolayer and nonpolar VOC. In other words, the electrical features of the Si NW FET device per se (μ_h, V_{th}, *etc.*) have lesser effect on the sensing process. To validate this claim, the change of the surface-state density ($n_s - n_{s0}/n_{s0}$) for the three different devices (*cf.* Supporting Information, Table 2S) upon exposure to hexane, octane, and decane was calculated (see Figure 8). As could be seen in the figure, for each VOC, the calculated $n_s - n_{s0}/n_{s0}$ values for the different devices were identical, disregarding the initial μ_h *and* V_{th}. An interesting observation from Figure 8 is that the longer the chain of the nonpolar VOC (*i.e.*, decane > octane > hexane), the higher the obtained response per 1 ppm (see Figure 8). It is reasonable to assume that the longer the nonpolar VOC, the higher the conformational disorder within the (HTS) monolayer, and the higher the response.

CONCLUSIONS

We have presented experimental evidence that nonpolar VOCs could be detected with improved sensitivity using a proper surface modification of Si NW FETs. Our results indicate that sensing nonpolar VOCs could be ascribed to adsorption of nonpolar VOCs between or on top of the chains and/or in the pinholes of the adsorptive monolayer. We speculate that this adsorption process induces conformational changes in the organic monolayer and affects the dielectric constant, the effective dipole moment of the organic monolayer, and/or the charged surface-state density of the SiO_2/monolayer interface. These effects, in turn, change the conductivity of the Si NW. Setting apart the water response is a major step toward the development of Si NW FETs for the development of a cost-effective, lightweight, low-power, noninvasive tool for the widespread detection of real-world VOCs in environmental, security, food, or medical[25−27] applications. Still, more research with different chain lengths of the functionality of the Si NWs is required in order to fully understand and confirm the observed results.

METHODS

The investigated Si NWs in this study were prepared by the vapor−liquid−solid growth technique, yielding p-type (111) Si NWs doped with boron to a doping level of $\sim 10^{16}$ cm^{-3}.[28] Transmission electron microscopy (TEM) data indicated that these Si NWs consisted almost entirely of smooth Si cores (~60 nm in diameter) coated with a ~5 nm native SiO_2 layer (see Figure 1c). Devices were fabricated by integrating an individual Si NW with source and drain Au/Ti electrodes (10 nm Ti and 100 nm Au) that were mutually separated by 2 μm on top of a 100 nm thermally oxidized degenerately doped p-Si (0.001Ω cm resistivity) substrate (see Figure 1a and b). The devices were functionalized with a stable 0% cross-linked hexyltrichlorosilane monolayer using the two-step amine-promoted reaction procedure described elsewhere.[19−21] This monolayer was shown to passivate a majority of oxide surface states and to result in a stable, reproducible, and minimal drift and/or hysteresis for Si NW FETs upon exposure to humidity.

The response of the Si NW FETs upon exposure to a series of nonpolar VOCs (hexane, octane, and decane; see Table 1) as well as to a series of polar VOCs (water, ethanol, butanol, and hexanol; see Table 1) was examined. For this purpose, a probe station that is connected to a device analyzer (Agilent B1500A) was used to collect the electrical signals of the Si NW FETs before and/or after exposure to VOCs. Voltage-dependent back-gate measurements ($I_{ds}-V_{gs}$), swept backward between +40 and −40 V with 200 mV steps and at 1 V source−drain voltage (V_{ds}), were used to determine the performance of Si NW FET sensors. For achieving the latter, oil-free air having 15% relative humidity and <0.3 ppm organic contamination was passed through a glass bubbler containing a liquid phase of the VOC of interest (purchased from Sigma Aldrich Ltd. and Fluka Ltd., having >99% purity and <0.001% water). The air emitted from the bubblers, mostly under saturation conditions, was diluted with oil-free air to reach lower levels of VOC concentrations. This way, the system was able to regulate the VOC concentration levels between $P_a/P_o = 0.0001$ and $P_a/P_o = 0.1$ (Note: P_a and P_o stand for the partial pressure and the saturated vapor pressure of the analytes, respectively). The concentration levels of VOCs were measured by a commercial photoionization detector (PID; ppbRAE 3000; Rae Systems, US), having a detection limit of ~10 ppb. In order to ensure referenced data, after each exposure cycle each device was cleaned with a 5 min flow and 10 min sonication cleaning with chloroform and 12 h drying in an 80 °C vacuum oven. Restoring the base (*i.e.*, before exposure) $I_{ds}-V_{gs}$ as the reference starting point after each sensing procedure, for an overall period of 6 months, has not affected its performance nor caused a device drift.

Acknowledgment. We acknowledge the financial support from the Marie Curie Excellence Grant of the FP6- and FP7-HEALTH Programs of the European Commission and the U.S.-Israel Binational Science Foundation. We acknowledge O. Assad (Technion) for assistance and G. Konvolina and U. Tisch (Technion) for constructive comments on the manuscript. H.H. is a Knight of the Order of Academic Palms

and holds the Horev Chair for Leaders in Science and Technology.

Supporting Information Available: Pre-factor shape at high negative voltages; summary of the relative responses of pristine and HTS-Si NW FETs to various analytes at the same concentration; and summary of the three devices' characteristics before and after response to different nonpolar VOCs at different concentrations. This material is available free of charge *via* the Internet at http://pubs.acs.org.

REFERENCES AND NOTES

1. Tisch, U.; Haick, H. Nanomaterials for Cross-Reactive Sensor Arrays. *MRS Bull.* **2010**, *35*, 797.
2. Patolsky, F.; Lieber, C. M. Nanowire Nanosensors. *Mater. Today* **2005**, *8*, 20.
3. Patolsky, F.; Zheng, G.; Hayden, O.; Lakadamyali, M.; Zhuang, X.; Lieber, C. M. Electrical Detection of Single Viruses. *Proc. Natl. Acad. Sci.* **2004**, *101*, 14017–14022.
4. McAlpine, M. C.; Ahmad, H.; Wang, D.; Heath, J. R. Highly Ordered Nanowire Arrays on Plastic Substrates for Ultrasensitive Flexible Chemical Sensors. *Nat. Mater.* **2007**, *6*, 379–384.
5. Cui, Y.; Wei, Q.; Park, H.; Lieber, C. M. Nanowire Nanosensors for Highly Sensitive and Selective Detection of Biological and Chemical Species. *Science* **2001**, *293*, 1289–1292.
6. Peng, G.; Trock, E.; Haick, H. Detecting Simulated Patterns of Lung Cancer Biomarkers by Random Network of Single-Walled Carbon Nanotubes Coated with Non-Polymeric Organic Materials. *Nano Lett.* **2008**, *8*, 3631–3635.
7. Peng, G.; Tisch, U.; Haick, H. Detection of Nonpolar Molecules by Means of Carrier Scattering in Random Networks of Carbon Nanotubes: Toward Diagnosis of Diseases via Breath Samples. *Nano Lett.* **2009**, *9*, 1362–1368.
8. Zilberman, Y.; Tisch, U.; Shuster, G.; Pisula, W.; Feng, X.; Müllen, K.; Haick, H. Carbon Nanotube/Hexa-peri-hexabenzocoronene Bilayers for Discrimination Between Nonpolar Volatile Organic Compounds of Cancer and Humid Atmospheres. *Adv. Mater.* **2010**, *22*, 4317–4320.
9. Bennett, M. E.; Alexander, W. A.; Lu, J. W.; Troya, D.; Morris, J. R. Collisions of Polar and Nonpolar Gases with Hydrogen Bonding and Hydrocarbon Self-Assembled Monolayers. *J. Phys. Chem. C* **2008**, *112*, 17272–17280.
10. Fagas, G.; Greer, J. C. Ballistic Conductance in Oxidized Si Nanowires. *Nano Lett.* **2009**, *9*, 1856–1860.
11. Haick, H.; Hurley, P. T.; Hochbaum, A. I.; Yang, P.; Lewis, N. S. Electrical Characteristics and Chemical Stability of Non-Oxidized, Methyl-Terminated Silicon Nanowires. *J. Am. Chem. Soc.* **2006**, *128*, 8990–8991.
12. Bashouti, M. Y.; Tung, R. T.; Haick, H. Tuning Electrical Properties of Si Nanowire Field Effect Transistors by Molecular Engineering. *Small* **2009**, *5*, 2761–2769.
13. Haight, R.; Sekaric, L.; Afzali, A.; Newns, D. Controlling the Electronic Properties of Silicon Nanowires with Functional Molecular Groups. *Nano Lett.* **2009**, *9*, 3165–3170.
14. Nolan, M.; O'Callaghan, S.; Fagas, G.; Greer, J. C.; Frauenheim, T. Silicon Nanowire Band Gap Modification. *Nano Lett.* **2007**, *34*, 34–38.
15. Koleini, M.; Ciacchi, L. C.; Fernndez-Serra, M. V. Electronic Transport in Natively Oxidized Silicon Nanowires. *ACS Nano* **2011**, *5*, 2839–2846.
16. Bashouti, M. Y.; Stelzner, T.; Berger, A.; Christiansen, S.; Haick, H. Chemical Passivation of Silicon Nanowires with C1−C6 Alkyl Chains through Covalent Si−C Bonds. *J. Phys. Chem. C* **2008**, *112*, 19168–19172.
17. Bashouti, M. Y.; Stelzner, T.; Berger, A.; Christiansen, S.; Haick, H. Covalent Attachment of Alkyl Functionality to 50 nm Silicon Nanowires through Chlorination/Alkylation Process. *J. Phys. Chem. C* **2009**, *113*, 14823–14828.
18. Jie, J.; Zhang, W.; Peng, K.; Yuan, G.; Lee, C. S.; Lee, S.-T. Surface-Dominated Transport Properties of Silicon Nanowires. *Adv. Funct. Mater.* **2008**, *18*, 3251.
19. Paska, Y.; Haick, H. Controlling Surface Energetics of Silicon by Intermolecular Interactions between Parallel Self-Assembled Molecular Dipoles. *J. Phys. Chem. C* **2009**, *113*, 1993–1997.
20. Paska, Y.; Haick, H. Controlling Properties of Field Effect Transistors by Intermolecular Cross-linking of Molecular Dipoles. *Appl. Phys. Lett.* **2009**, *95*, 233103/1–233103/3.
21. Paska, Y.; Haick, H. Systematic Cross-Linking Changes within a Self-Assembled Monolayer in a Nanogap Junction: A Tool for Investigating the Intermolecular Electronic Coupling. *J. Am. Chem. Soc.* **2010**, *132*, 1774–1775.
22. Wunnicke, O. Gate Capacitance of Back-Gated Nanowire Field-Effect Transistors. *Appl. Phys. Lett.* **2006**, *89*, 083102.
23. Natan, A.; Kronik, L.; Haick, H.; Tung, R. T. Electrostatic Properties of Ideal and Non-Ideal Polar Organic Monolayers: Implications for Electronic Devices. *Adv. Mater.* **2007**, *19*, 4103–4117.
24. Gao, X. P. A.; Zheng, G.; Lieber, C. M. Subthreshold Regime has the Optimal Sensitivity for Nanowire FET Biosensors. *Nano Lett.* **2010**, *10*, 547–552.
25. Peng, G.; Hakim, M.; Broza, Y. Y.; Billan, S.; Abdah-Bortnyak, R.; Kuten, A.; Tisch, U.; Haick, H. Detection of Lung, Breast, Colorectal, and Prostate Cancers from Exhaled Breath Using a Single Array of Nanosensors. *Br. J. Cancer* **2010**, *103*, 542–551.
26. Peng, G.; Tisch, U.; Adams, O.; Hakim, M.; Shehada, N.; Broza, Y. Y.; Billan, S.; Abdah-Bortnyak, R.; Kuten, A.; Haick, H. Diagnosing Lung Cancer in Exhaled Breath using Gold Nanoparticles. *Nat. Nanotechnol.* **2009**, *4*, 669–673.
27. Hakim, M.; Billan, S.; Tisch, U.; Peng, G.; Dvrokind, I.; Marom, O.; Abdah-Bortnyak, R.; Kuten, A.; Haick, H. Diagnosis of Head&Neck Cancer from Exhaled Breath. *Br. J. Cancer* **2011**, *104*, 1649–1655.
28. Stelzner, T.; Andra, G.; Wendler, E.; Wesch, W.; Scholz, R.; Goesele, U.; Christiansen, S. Growth of Silicon Nanowires by Chemical Vapor Deposition on Gold Implanted Silicon Substrates. *Nanotechnology* **2006**, *17*, 2895–2898.
29. Haynes, W. M. *CRC Handbook of Chemistry and Physics*, 91st ed.; CRC Press: Boulder, CO, 2010−2011.